ADVANCES IN ATMOSPHERIC SCIENCES, VOL. 25, NO. 5, 2008, 867–884

Statistical Downscaling for Multi-Model Ensemble Prediction of Summer Monsoon Rainfall in the Asia-Pacific Region Using Geopotential Height Field

ZHU Congwen*[1,2] (祝从文), Chung-Kyu PARK[2], Woo-Sung LEE[4], and Won-Tae YUN[3]

[1] *Chinese Academy of Meteorological Sciences, Beijing* 100081

[2] *Asia-Pacific Economic Cooperation Climate Center (APCC), Busan, Republic of Korea*

[3] *Korea Meteorological Administration, Seoul, Republic of Korea*

[4] *Canadian Centre for Climate Modelling and Reanalysis, Victoria, BC, Canada*

(Received 2 August 2007; revised 27 February 2008)

ABSTRACT

The 21-yr ensemble predictions of model precipitation and circulation in the East Asian and western North Pacific (Asia-Pacific) summer monsoon region (0°–50°N, 100°–150°E) were evaluated in nine different AGCM, used in the Asia-Pacific Economic Cooperation Climate Center (APCC) multi-model ensemble seasonal prediction system. The analysis indicates that the precipitation anomaly patterns of model ensemble predictions are substantially different from the observed counterparts in this region, but the summer monsoon circulations are reasonably predicted. For example, all models can well produce the interannual variability of the western North Pacific monsoon index (WNPMI) defined by 850 hPa winds, but they failed to predict the relationship between WNPMI and precipitation anomalies. The interannual variability of the 500 hPa geopotential height (GPH) can be well predicted by the models in contrast to precipitation anomalies. On the basis of such model performances and the relationship between the interannual variations of 500 hPa GPH and precipitation anomalies, we developed a statistical scheme used to downscale the summer monsoon precipitation anomaly on the basis of EOF and singular value decomposition (SVD). In this scheme, the three leading EOF modes of 500 hPa GPH anomaly fields predicted by the models are firstly corrected by the linear regression between the principal components in each model and observation, respectively. Then, the corrected model GPH is chosen as the predictor to downscale the precipitation anomaly field, which is assembled by the forecasted expansion coefficients of model 500 hPa GPH and the three leading SVD modes of observed precipitation anomaly corresponding to the prediction of model 500 hPa GPH during a 19-year training period. The cross-validated forecasts suggest that this downscaling scheme may have a potential to improve the forecast skill of the precipitation anomaly in the South China Sea, western North Pacific and the East Asia Pacific regions, where the anomaly correlation coefficient (ACC) has been improved by 0.14, corresponding to the reduced RMSE of 10.4% in the conventional multi-model ensemble (MME) forecast.

Key words: summer monsoon precipitation, multi-model ensemble prediction, statistical downscaling forecast

Citation: Zhu, C. W., C.-K. Park, W.-S. Lee, and W.-T. Yun, 2008: Statistical downscaling for multi-model ensemble prediction of summer monsoon rainfall in the Asia-Pacific region using geopotential height field. *Adv. Atmos. Sci*, **25**(5), 867–884, doi: 10.1007/s00376-008-0867-x.

1. Introduction

The East Asian and western North Pacific monsoon (Asia-Pacific monsoon) is a complex system that affects global climate. It is characterized not only by unique seasonal changes, but also by the remarkable interannual variability of the winter and summer monsoons (Tao and Chen, 1987; Wang and Fan, 1999; Wang et al., 2001a; Li and Zeng, 2002; Zhu et al., 2005, and among others). The prediction ability of General

*Corresponding author: ZHU Congwen, tomzhu@cams.cma.gov.cn

Circulation Models (GCMs) on the seasonal time-scale has been improved, however, the model forecast skill varies from region to region (Brankovic et al., 1994), and the model has almost no skill in the prediction of monsoon seasonal climate anomalies (Palmer et al., 2000).

Wang et al. (2001b) examined the performance of a coupled GCM (CGCM) on seasonal to interannual prediction focusing on SST fields, model biases and forecast skill. They found that the coupled model is capable of simulating the basic ENSO features in the tropical Pacific, but the precipitation patterns are weak and somewhat shifted in the mid-latitudes of the Asian Pacific region. The insufficient predictions in the variations of summer monsoon rainfall over the Asian-Western Pacific region and the systematic errors also exist in a number of AGCMs, where the observed meiyu rain band from the East China Sea to the central Pacific could not be reproduced (Kang et al., 2002). On the basis of predictions in 11 AGCMs, Wang et al. (2004) evaluated the model predictions of summer rainfall anomaly in the Asian-Australian (A-A) monsoon regions (30°S–30°N, 40°–160°E). They found the model-predicated rainfall patterns are less realistic in the A-A monsoon regions, which is mainly due to the lack of skill over Southeast Asia and the western North Pacific (WNP) (5°–30°N, 80°–150°E). Therefore, the current model atmosphere in the mid-latitudes does not respond correctly to tropical sea surface temperature (SST) forcing, particularly over the Asia-Pacific summer monsoon region.

A number of studies have shown that the limitations of dynamical predictions are not only due to the inherent nonlinear characteristics of the atmosphere, but also the inaccurate responses of current GCMs to external forcings, and that they mainly come from the SST anomalies (Sperber and Palmer, 1996; Goswami, 1998; Feddersen et al., 1999; Sperber et al., 2001; Wang et al., 2004; Kang et al., 2004). This kind of model bias in the external component appears in a systematic way in both the climatological mean and the anomalies. The major part of the systematic error associated with the anomaly component, predominantly forced by the SST anomalies, can be corrected by using a statistical relationship between the prediction and observed anomalies based on EOF, canonical correlation analysis (CCA), and singular value decomposition (SVD) as well (Feddersen et al., 1999; Kang et al., 2004). In order to reduce both model systematic error and uncertainties in initial conditions, a new approach to weather and climate forecasts, called the multi-model ensemble (MME) method was recently proposed (Palmer et al., 2000). The basic idea of MME is to avoid model inherent error by using a number of independent and skillful models in the hope of a better coverage of all of the possible climate phase spaces (Hagedorn et al., 2005). Similar to statistical downscaling schemes, the transfer functions linking the model forecast and the observed atmospheric variables have been widely applied to the MME forecasts. However, the basic assumptions of statistical downscaling are that the predictors are reliable, and that the derived transfer functions are stable in time (Charles et al., 1999; Wilby and Wigley, 2000). Therefore, the tasks of the downscaling scheme and MME forecasts are not only to find the transfer functions, where the predictors strongly correlated with the predictands, but also to identify those predictors that can be well forecasted by model. It is noted that a related problem here is the stability of the regression equation for the different training and forecast time periods. If the relationships have a sound physical basis, however, they are more likely to remain stable in time.

Because of the marginal performance of current climate models in forecasting the Asia-Pacific summer monsoon rainfall, this study uses other prognostic variables as the predictor to predict the Asia-Pacific summer monsoon rainfall anomaly. In this study, we proposed a statistical downscaling method, where the 500 hPa geopotential height is chosen as a predictor, and used to predict the Asia-Pacific summer monsoon precipitation by SVD. This scheme is built on the basis of verification of the model hindcasts and the relationship between the observed summer monsoon circulation and precipitation anomalies. The MME prediction is defined as a joint ensemble mean of 9 model forecasts used in the present study.

In the remainder of this paper, model predictions and observed data used in the present study are described in section 2. The verifications of model predictions for the Asia-Pacific summer monsoon circulation and precipitation anomalies are presented in section 3. The physical basis applied to the statistical downscaling scheme in this study is explored in section 4. The statistical downscaling scheme and its forecast skill scores for individual model and conventional MME forecasts are discussed in terms of anomaly correlation coefficient (ACC), RMSE, and temporal correlation between downscaled and observed precipitation anomalies in section 5. A summary and conclusions are given in section 6.

2. Data sets

The Atmospheric Model Intercomparison Project (AMIP), Seasonal Prediction Model Intercomparison Project-2 (SMIP2), and Historical Forecasting Project (HFP) have provided comprehensive evaluations of the

Table 1. The acronym and descriptions of models used in the text, tables, and figures in this study.

Acronym	Ensemble Size	Resolution	Hindcast Type	Member Economy	Full name/participating institution
CWB	5	T42, L18	SMIP	Chinese Taipei	Central Weather Bureau
GCPS	6	T63, L21	SMIP/HFP	Korea	Global Climate Prediction System/Korea Meteorological Administration
GDAPS	10	T106, L21	SMIP	Korea	Global Data Analysis and Prediction System/Korea Meteorological Administration
HMC	6	1.125×1.406, L28	SMIP/HFP	Russia	Hydrometeorological Centre of Russia
IRI	24	T42, L18	AMIP	United States	International Research Institute for Climate Prediction
JMA	6	T63, L40	SMIP	Japan	Japan Meteorological Agency
METRI	10	4×5, L17	SMIP/HFP	Korea	Meteorological Research Institute/Korea Meteorological Administration
MGO	6	T42, L14	SMIP	Russia	Main Geophysical Observatory
NCEP	10	T62, L64	SMIP	United States	Climate Prediction Center/National Centers for Environmental Prediction

performance of atmospheric GCMs, which have proven to be useful benchmarks of model sensitivity and predictability experiments to SST forcing (Slingo et al., 1996; Sperber et al., 2001). In the AMIP-type experiment, an AGCM is constrained by realistic SST and sea ice; however, the SMIP2-type experiment is to investigate the first and second season potential predictability based on initial conditions and the AGCM response to specified observed values of SST and sea-ice. In the SMIP2/HFP-type experiment, the models' first season actual predictability is based on initial conditions and the AGCM response to predicted values of SST and sea-ice. Also, it may be based on the results of a coupled atmosphere-ocean forecast system (Sperber et al., 2001; Kusunoki et al., 2001).

Table 1 shows the 9 models utilized in this study, where the predictions in all models are based on the SMIP2 or SMIP2/HFP-type experiment except the model of IRI, the prediction in this model is designed based on the type of AMIP. The outputs of model prediction utilized consist of 21-yr ensemble and summer season-averaged models' predictions. The variables used are precipitation, 500 hPa geopotential height (hereafter, 500 hPa GPH), winds and the temperature at 850 hPa for boreal summer (June to August) during 1979–1999. The observed precipitation data used in this study are from the Climate Prediction Center (CPC) Merged Analysis of Precipitation (CMAP) dataset (Xie and Arkin, 1997). The 2.5° × 2.5° of spatial resolution in CMAP is coarse for downscaling study, however, it is the only candidate data covering land and ocean with a long enough record; the other observed atmospheric variables corresponding to the model predictions were constructed from the NCEP-DOE AMIP-II Reanalysis (R-2) (Kanamitsu et al., 2002). These observations are used to assess the model forecasting skills and investigate the transfer function between the summer monsoon circulation and the precipitation anomaly. All data sets used in this study are on the 2.5° by 2.5° grid.

3. Asia-Pacific summer monsoon forecasts by the models

The model forecasting skills in the Asia-Pacific summer monsoon region are evaluated by computing correlation coefficients between the observed and model-forecasted anomaly fields, which measures the point-to-point correlation between the two fields during the 21-yr hindcast period. Meanwhile, to examine the year-to-year variations of model rainfall anomaly forecasting skill scores in the Asia-Pacific summer monsoon region of 0°–50°N, 100°–150°E, we calculated the ACC and RMSE in each model prediction

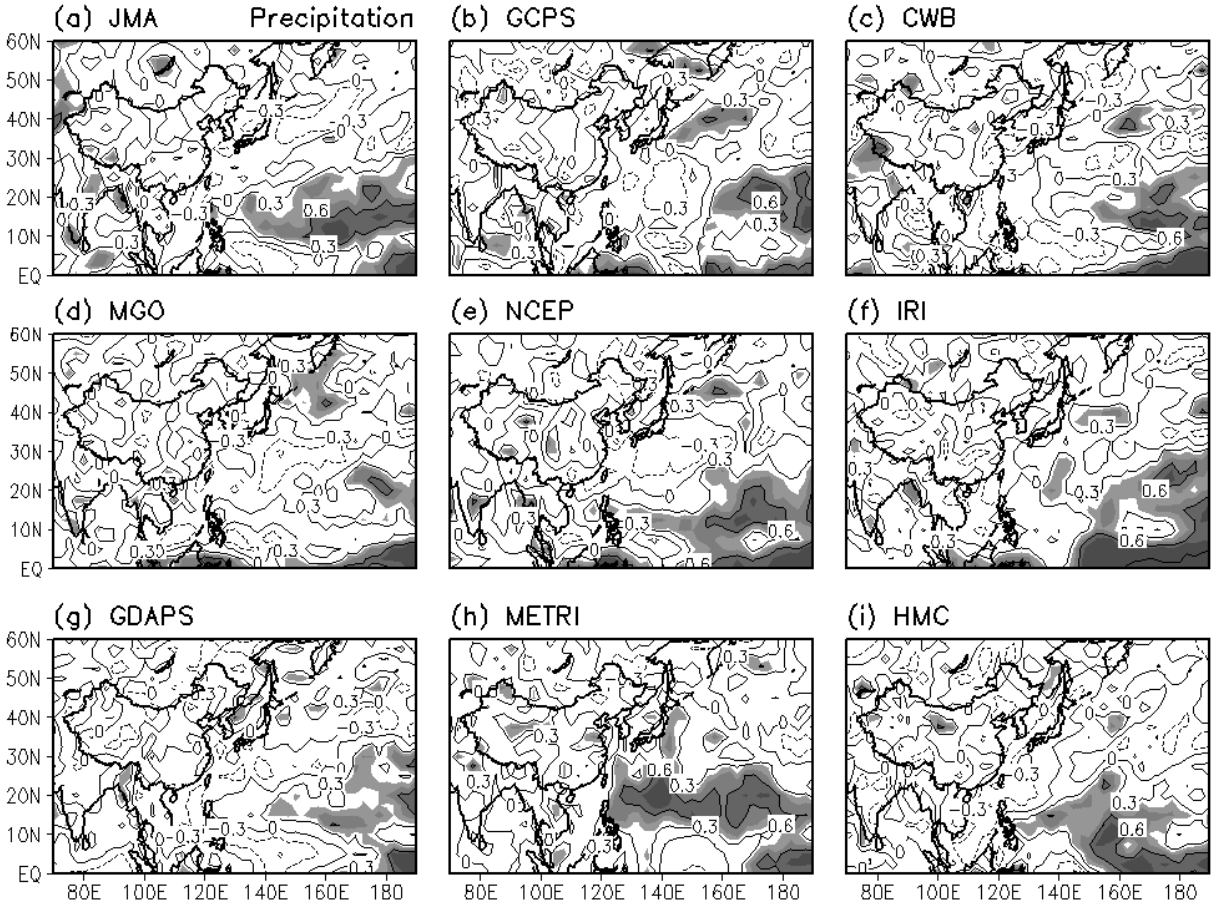

Fig. 1. Correlation coefficients between observed and model-predicted precipitation anomaly during summer of 1979–1999 for (a) JMA, (b) GCPS, (c) CWB, (d) MGO, (e) NCEP, (f) IRI, (g) GDAPS, (h) METRI, and (i) HMC models. Contour interval is 0.3. The shaded indicates the correlations passed 0.05 significant test levels.

and MME scheme, and used them to measure the simultaneous spatial correlation and bias between observation and model prediction with the sample size, which is determined by the total number of grids in the given region.

Figure 1 shows the spatial distributions of temporal correlation coefficients between observation and model summer precipitation anomalies during the model hindcast period of 1979–1999. It is noted that positive correlations with 95% confidence level are found only in the tropical western Pacific regions (0°–30°N, 120°–180°E) in the models. These regions are corresponding to the sectors with higher potential predictability in the dynamical models as discussed by Kang et al. (2004). In the region of (0°–50°N, 100°–150°E), including from the South China Sea (SCS) to the eastern Philippine Sea, the sector from Yangtze River to the southern islands of Japan, and the major parts of WNP, the models show weaker or even negative correlations. Thus, the model precipitations are not convincing and could not be directly applied in the seasonal forecast in these summer monsoon regions.

Figure 2 shows the interannual variability of the ACC and RMSE of each model and MME scheme for the region of (0°–50°N, 100°–150°E). It was found the models show a higher ACC in the case of 1981 and 1995 for example, however, the general skills indicated by the 21-yr averaged ACC are still very low, and even show negative values. Also, the ACC is less than 0.1 in 7 of the 9 models. The higher ACC is 0.18 in METRI and 0.11 in IRI. In MME scheme, the ACC is only 0.07. The rainfall anomaly forecast skill of MME scheme is relatively better, but it is still poor due to weaker individual model performance in this region. The MME scheme shows the smaller bias in the year-to-year variations of RMSE, the 21-yr averaged RMSE in the model and MME scheme ranges from 1.73 to 2.32 mm d^{-1}, and the MME is smaller than any other model biases. Several models show better skills with the higher ACC and lower RMSE, but they failed to predict the summer monsoon rain band anomalies as it was shown in Fig. 1.

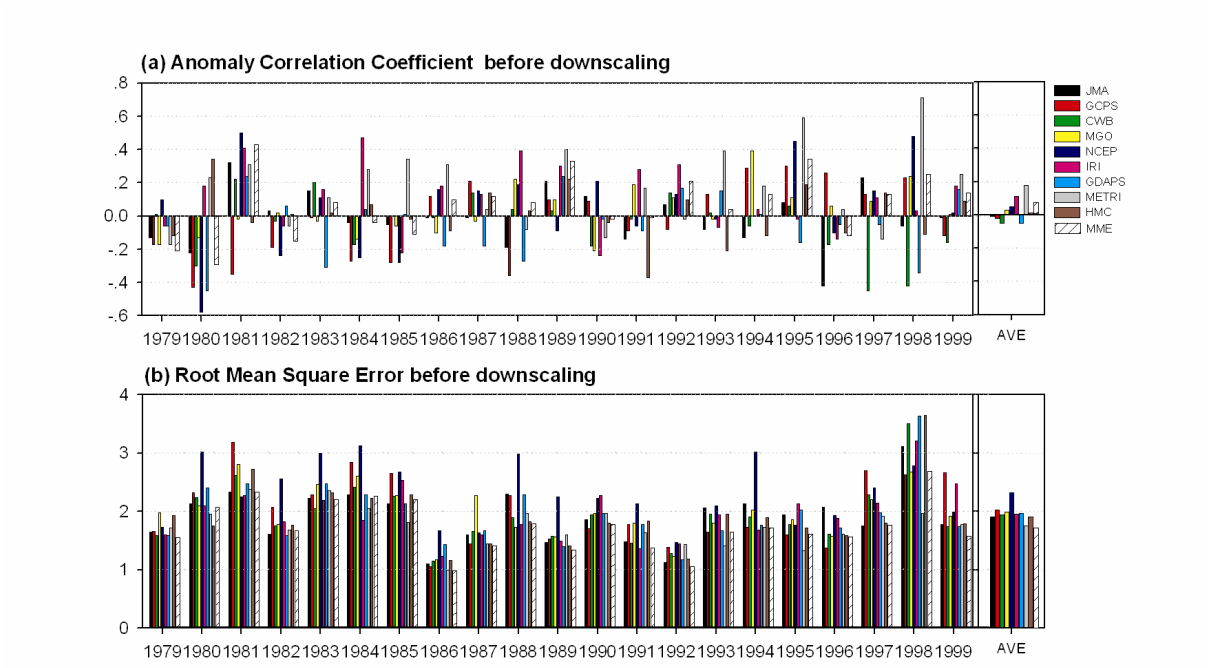

Fig. 2. The interannual variability of the precipitation anomaly forecast skill scores for each model and MME scheme in the Asia-Pacific summer monsoon region of (0°–50°N, 100°–150°E), which are evaluated by (a) spatial anomaly correlation, and (b) root mean square error between observation and models' predictions during 1979–1999. The averaged forecast skill scores are presented in the last column in the figures.

In contrast to the precipitation anomaly forecast, the models show better performance in forecasting the 500 hPa GPH anomaly field (Fig. 3). The correlation coefficients between the observed and model-predicted 500 hPa GPH anomaly field range from 0.2 to 0.8, and such positive correlations cover most areas with the exception of the sectors from the Yangtze River valley to the southern islands of Japan, which are dominated by the summer mei-yu (Changma in Korean, Baiu in Japanese) rain belts. In addition, it was found the models also show better skill in predicting temperature and zonal wind at 850 hPa in terms of correlation analysis (the figures are not shown). This evidence implies the models have better skill in the Asia-Pacific summer monsoon circulation forecast compared to the case of precipitation anomaly.

The previous studies have shown that the interannual variability of the western North Pacific monsoon index (WNPMI, Wang and Fan, 1999; Wang et al., 2001a) has a good capability in representing East

Table 2. Correlation coefficients between observed and model-forecasted western North Pacific monsoon index of WNPMI (Wang and Fan, 1999; Wang et al., 2001a) by 8 participating models during 1979–1999; The marked correlation coefficients by one and two asterisk represents the correlations which passed the 0.05 and 0.01 significance testing, respectively. The METRI is excluded due to the absent 850 hPa wind vectors in the present study.

	Correlation coefficient								
	OBS.	JMA	GCPS	CWB	MGO	NCEP	GDAPS	IRI	HMC
OBS.	1.0	0.58*	0.48*	0.56*	0.51*	0.78**	0.59*	0.43*	0.71**
JMA		1.0	0.40	0.68**	0.49*	0.69**	0.85*	0.37	0.62*
GCPS			1.0	0.46*	0.72**	0.56*	0.12	−0.05	0.23
CWB				1.0	0.76**	0.70**	0.65*	0.43*	0.62*
MGO					1.0	0.58*	0.46*	0.13	0.45*
NCEP						1.0	0.57*	0.44*	0.53*
GDAPS							1.0	0.43*	0.65**
IRI								1.0	0.61*
HMC									1.0

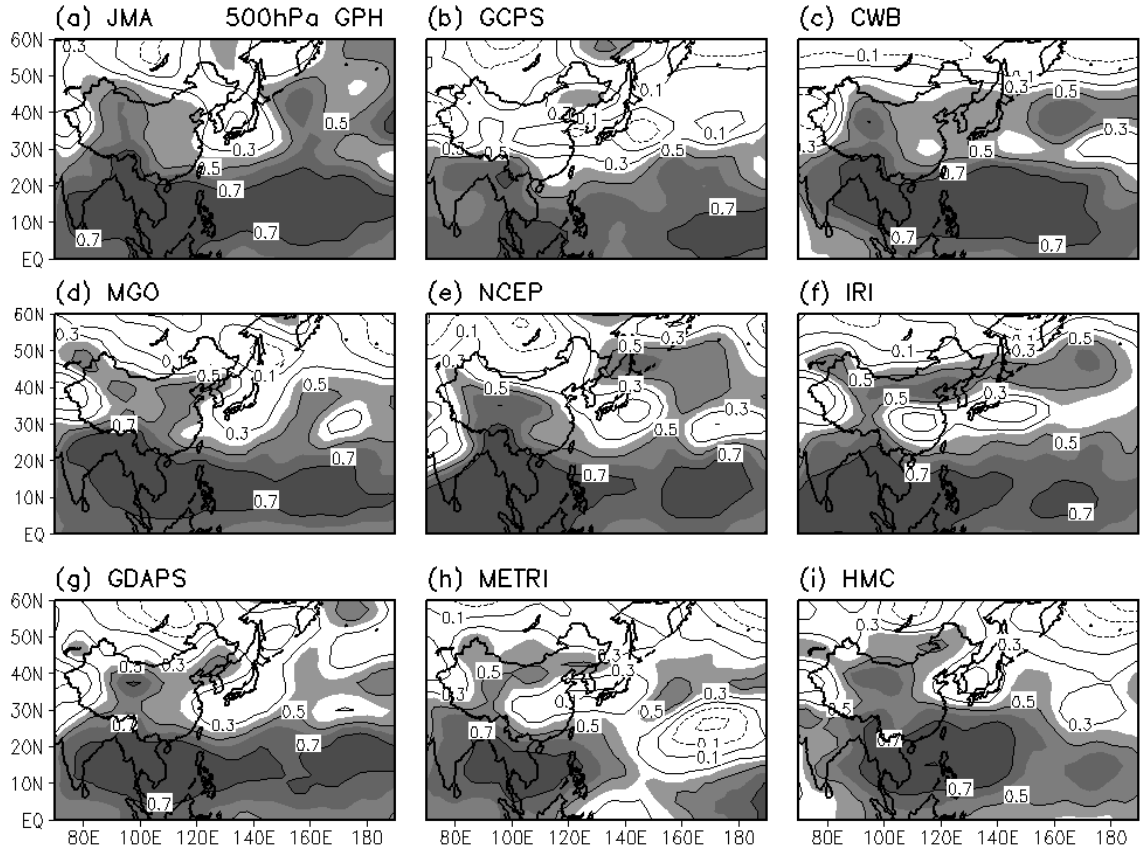

Fig. 3. Same as Fig. 1, but for the 500 hPa GPH anomaly fields. Contour interval is 0.2 and the zero contours are omitted.

Asian and western North Pacific summer monsoon circulation and precipitation anomaly patterns (Zhu et al., 2005). We applied the WNPMI to examine the model performances in predicting the Asia-Pacific summer monsoon circulation and the relationship with the model precipitation anomalies following the previous study (Wang et al., 2004). Table 2 shows the correlation coefficients of WNPMI between the observation and the model prediction. It is found that all models can predict the WNPMI well, and the correlation coefficients of WNPMI are greater than 0.42 and reach a maximum of 0.78, which exceed the 0.05 significance level.

Corresponding to the positive WNPMI, it was shown that the summer rainfall is enhanced over the SCS, the eastern Philippine Sea to the south, and over the Okhotsk Sea to the north, while the mei-yu rainfall pattern is suppressed from the mid-lower reaches of the Yangtze River to the southern Japanese Islands (Zhu et al., 2005). Such a monsoon rainfall pattern had been widely addressed by many studies (e.g., Nitta, 1987; Nitta and Hu, 1996; Wang et al., 2001a; Li and Zeng, 2002; Zhu et al., 2005). A recent study shows that this monsoon pattern anomaly is a response of the Asia-Pacific summer monsoon to the atmosphere external forcing of ENSO-related SST anomaly (Lee et al., 2005). To examine the relationship between model-forecasted monsoon circulation and precipitation anomaly, we calculated the correlations between WNPMI and precipitation anomaly for the observation and each model prediction and presented these results in Fig. 4.

The correlation between the model-forecasted WNPMI and the precipitation anomaly field shows positive correlation coefficients over the region of the SCS to the eastern Philippine Sea, where the maximum correlation coefficients reach 0.8 in some of the models. However, in the mid-lower reaches of the Yangtze River to the southern islands of Japan and the Okhotsk Sea to the north, the high correlation coefficients between WNPMI and rainfall anomalies with respect to the observations are not found in the models' predictions. The correlations shift greatly in contrast to the observed case, therefore the models failed to predict the correct relationship between the summer monsoon circulation and rainfall anomaly field due to the unrealistic rainfall anomaly predictions in the middle-high latitudes of the Asia-Pacific region.

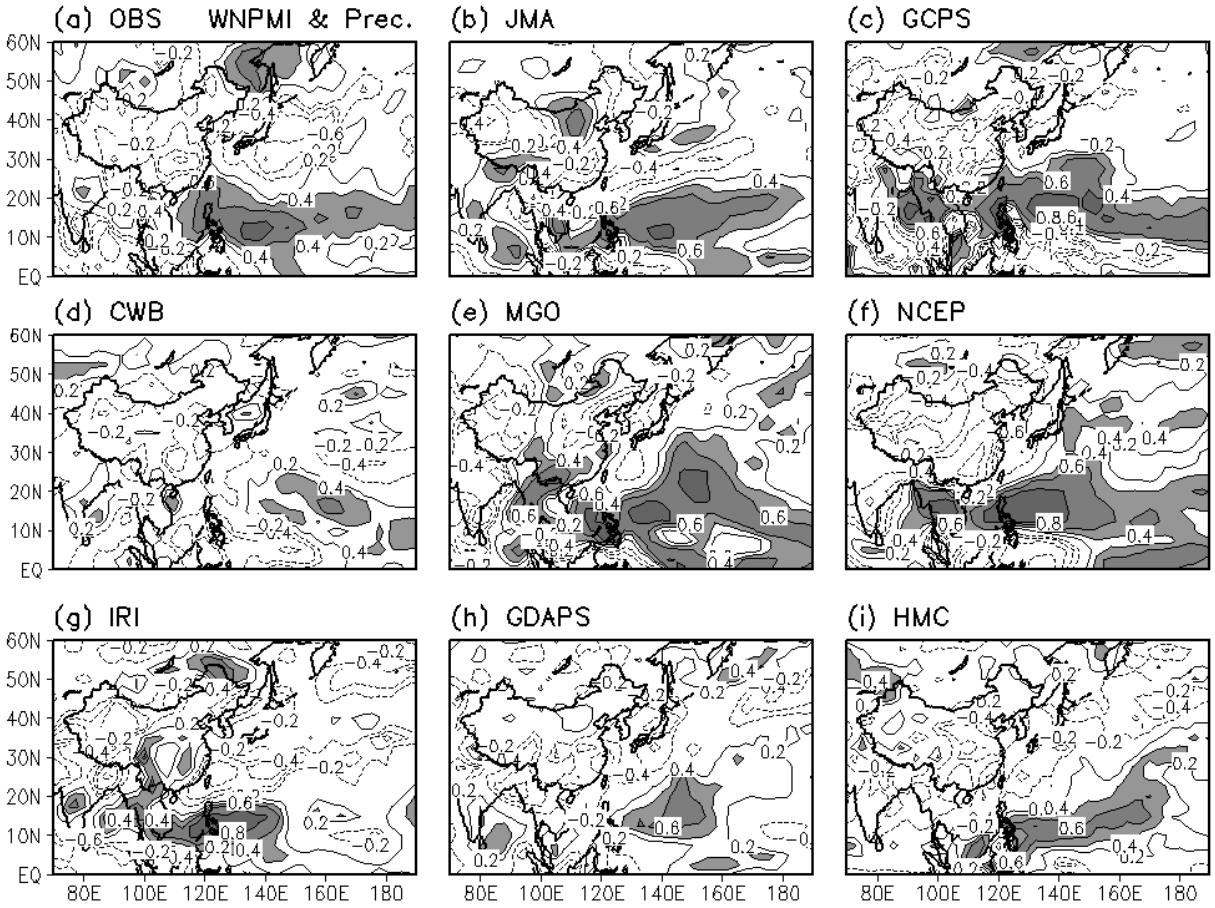

Fig. 4. The correlation coefficients between the western North Pacific monsoon index (WNPMI) and the precipitation anomaly for (a) observation, (b) JMA, (c) GCPS, (d) CWB, (e) MGO, (f) NCEP, (g) IRI, (h) GDAPS, and (i) HMC. Contour interval is 0.2, the zero contours are omitted, and the regions where the values greater than 0.2 are shaded.

Many studies have addressed the issue of the weak model forecasting skill of the summer monsoon rainfall (e.g., Wang et al., 2001b; Kang et al., 2004), however, it is worth noting that the weak model rainfall forecasting skill might come from the improper parameterization scheme in the middle-high latitudes rather than the incorrect responding of summer monsoon circulation to the external forcing due to the existing higher correlations between the observed and the model-predicted WNPMI and partially correct rainfall pattern prediction over the SCS to the eastern Philippine Sea.

4. Coupling between summer monsoon rainfall and 500 hPa GPH

The better skill of the models in predicting the year-to-year variations of the summer monsoon circulation anomaly and 500 hPa GPH shows us the potential information in the model predictions, which can possibly be used to improve the rainfall anomaly forecast if the sound relationship (transfer function) between the Asia-Pacific summer monsoon circulation and precipitation anomaly is clearly explored. In statistical downscaling, this kind of transfer function is mainly investigated by the EOF, CCA, and SVD techniques (e.g., Feddersen et al., 1999; Feddersen, 2003; Kang et al., 2004). However, the eigenmodes extracted by these methods might be quite different from region to region due to the varying covariance matrix, which is related to the local atmospheric internal variability and the responding to the boundary forcing, mainly from SST anomalies. In this study, we choose the 500 hPa GPH in the region of 0°–60°N, 70°E–170°W, which covers the Bay of Bengal, SCS to the eastern Philippine Sea, and the East Asian and western North Pacific summer monsoons, and discuss the creditable transfer function between the model-predicted 500 hPa GPH and the observed precipitation anomaly fields by virtue of EOF and SVD.

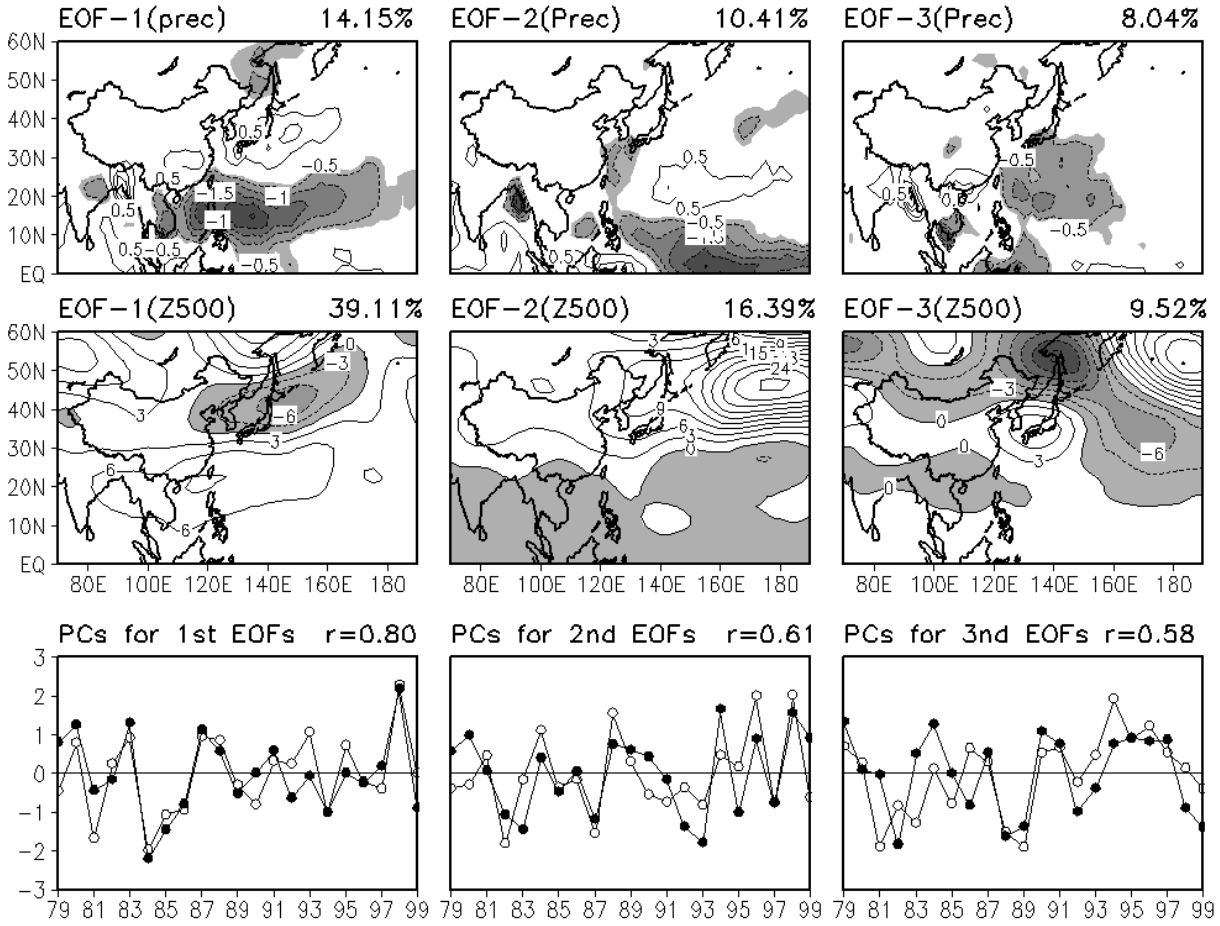

Fig. 5. The three leading EOF modes of the observed summer (June to August) precipitation anomaly (upper panels; contour interval is 0.5 where the values less than −0.3 are shaded), 500 hPa GPH (middle panels; contour interval is 3 where the negative values are shaded), and their corresponding PCs (bottom panels) during 1979–1999. The solid line with closed and open circle denotes the PC for 500 hPa GPH and precipitation anomaly, respectively. The right side of the bottom title line represents the correlation coefficient between PCs in the two fields.

Figure 5 shows the first three EOF modes corresponding to the observed summer precipitation and 500 hPa GPH anomaly fields during 1979–1999. The EOF mode of observed precipitation anomaly exhibits a similar triple pattern as we have seen in Fig. 4, but here it represents the dominant monsoon rainfall pattern related to the interannual variability of the Asia-Pacific summer monsoon rainfall anomaly. The first EOF of the observed 500 hPa GPH anomalies indicates the dominant monsoon circulation mode and shows that the similar triple pattern with opposite signs of centers compared to the counterpart of summer rainfall anomalies. The observed monsoon precipitation and circulation anomaly pattern exhibit a remarkable interannual variability and show a close relationship with the interannual variability of ENSO as indicated by the variations of corresponding principal components (PCs). For example, during the summer of 1983, 1987, 1993, and 1998 corresponding to the decaying phases of ENSO, the Asia-Pacific summer monsoon is weaker, and the rainfall over the low-middle reaches of the Yangtze River valley to southern islands of Japan (the SCS to the eastern Philippine Sea) were greatly enhanced (suppressed) corresponding to the enhanced western North Pacific subtropical high (WNPSH) centered over the SCS and the middle-latitude trough over the Eastern central Japanese Islands. The second and third EOFs of precipitation and 500 hPa GPH anomaly fields also exhibit a very consistent year-to-year variability, but the large variance corresponding to the EOF modes of precipitation anomalies move to the tropical and western North Pacific, respectively, associated with the counterparts of 500 hPa GPH anomalies in the middle-high latitudes over the East Asia-Pacific region.

The model-predicted spatial pattern of precipita-

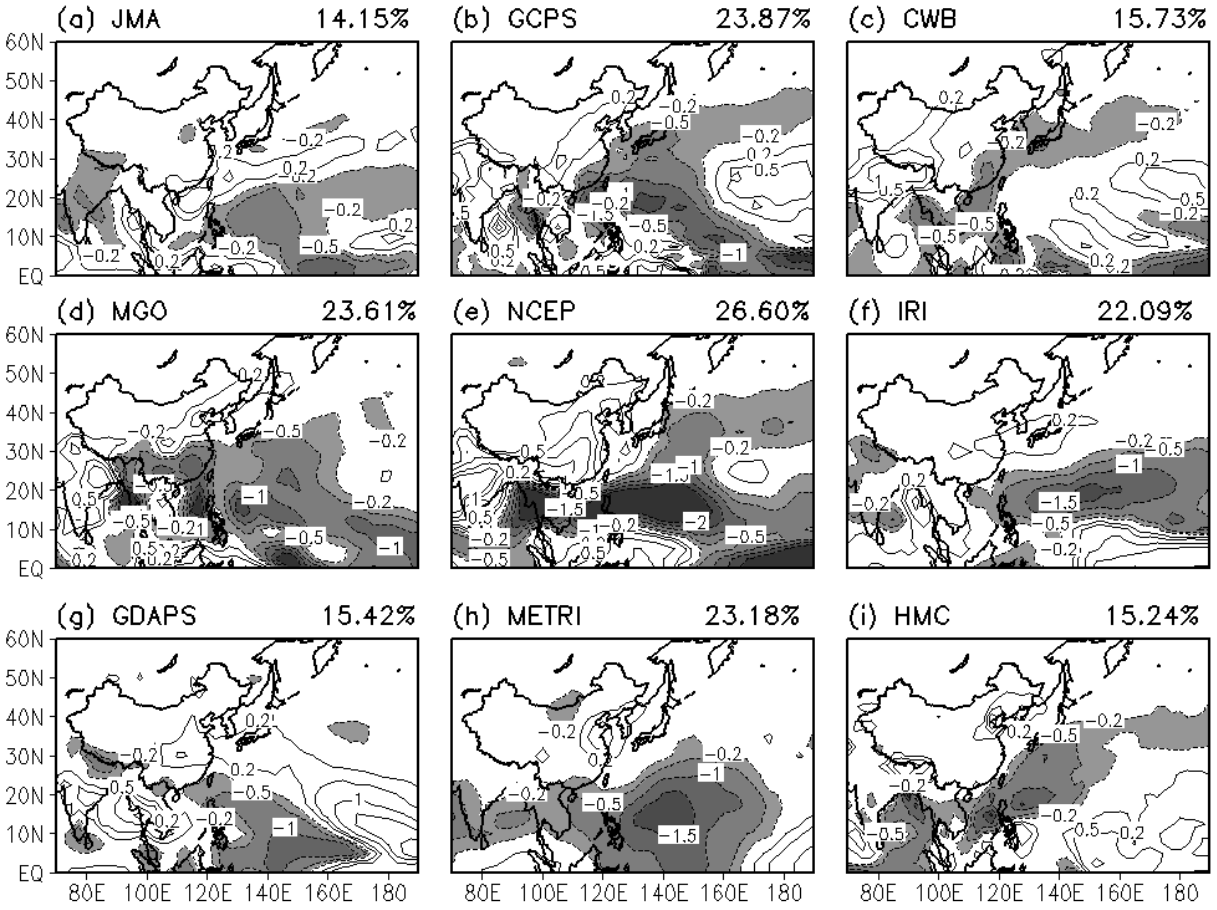

Fig. 6. The first EOF mode for the model-predicted summer precipitation anomaly during 1979–1999 in (a) JMA, (b) GCPS, (c) CWB, (d) MGO, (e) NCEP, (f) IRI, (g) GDAPS, (h) METRI, and (i) HMC models. Contour interval is 0.5, the values between −0.2 and 0.2 are omitted, and the regions where the values less than −0.2 are shaded. The variance explained by the EOF in each model is printed on the right side of the title line.

tion anomaly explored by the first EOF mode is different from the counterpart of observed precipitation anomaly (see Fig. 6), where the EOF showed the pattern either in a zonal or a meridional dipole in the models. The observed rainfall anomaly corresponding to the first EOF mode over the SCS to the eastern Philippine Sea can be observed in the counterpart of the model predictions, but the models failed to predict the rainfall anomalies in the middle-higher latitudes. The spatial pattern of the model-simulated 500 hPa GPH is not much better than the counterpart of precipitation anomaly, and the discrepancy between the observed and model-simulated EOF modes is still remarkable (see Fig. 7). Some of the models can simulate the overall anomaly pattern, but the systematic shift is still present. However, the transfer function between model prediction and observation is dependent on the linear relationship between expansion coefficients related to the model and observed EOF modes, if the dominant expansion coefficients corresponding to the leading eigenmodes can be well predicted by the model, the spatial discrepancies between observation and model prediction, however, can be corrected by replacing the model eigenmodes with the corresponding observed ones (e.g., Feddersen et al., 1999; Feddersen, 2003; Kang et al., 2004).

To examine how well the models can predict expansion coefficients corresponding to the spatial patterns, we calculated the correlations between the observed and model-predicted expansion coefficients associated with the three leading EOF modes of 500 hPa GPH and precipitation anomalies, respectively (see Table 3). The models show a good performance in predicting the interannual variability of PCs corresponding to the EOF modes of model 500 hPa GPH anomaly field. The correlations between the first pair of PCs passed the 95% and 99% confidence level with correlation coefficients varying from 0.46 to 0.79 in the models, and such a remarkable correlation can also be observed in the second pair of PCs in most models, and even in

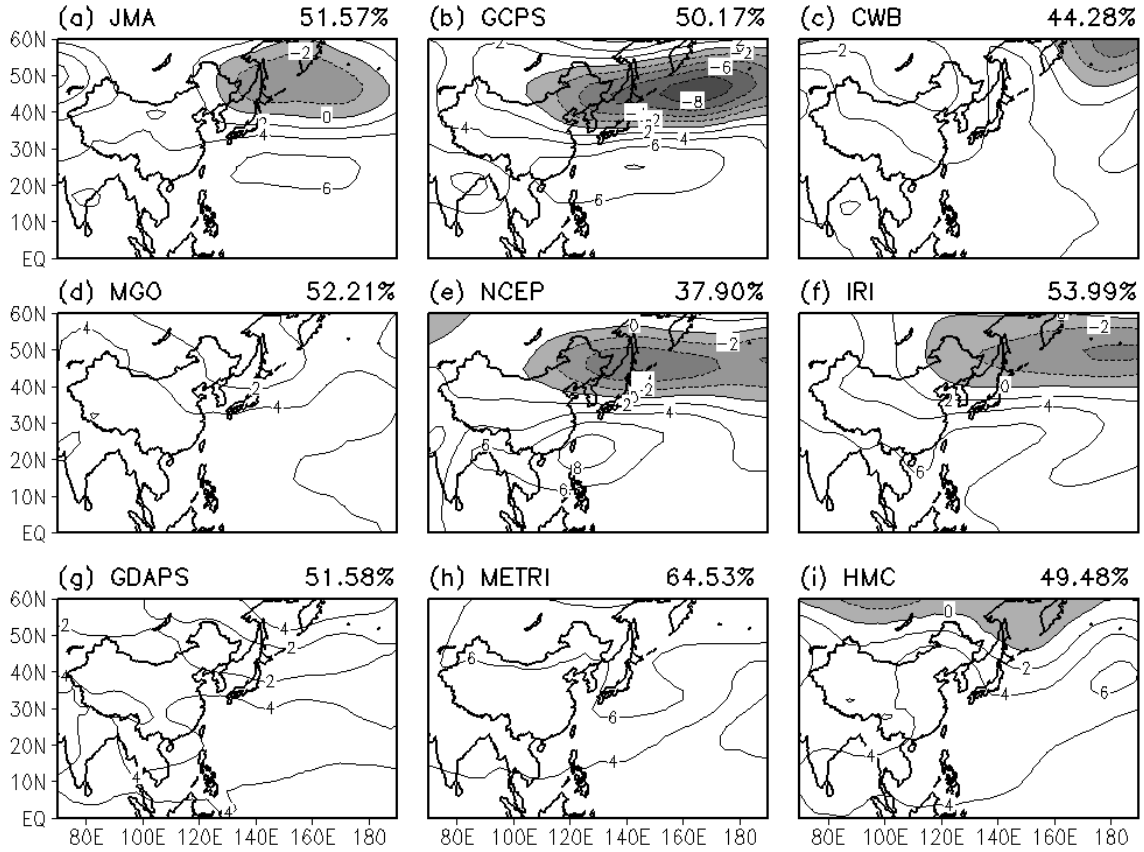

Fig. 7. Same as Fig. 6, except for the model-forecasted 500 hPa GPH anomaly field. Contour interval is 2 and the negative values are shaded.

the third pair of PCs in some models. In contrast, the absolute values of correlation coefficients for the first EOF of precipitation anomaly between observation and model predictions range from 0.04 to 0.65, where the correlation between the first pair of PCs in some models can pass the 0.05 significance level, but no remarkable correlations are found between the second and third pair of PCs in the model-simulated precipitation anomaly fields. As a result, the model-predicted 500 hPa GPH exhibits a better candidate of predictors, which can be used to downscale the precipitation anomaly if the relationship between the 500 hPa GPH and precipitation anomaly fields was clearly explored.

To address the relationship between the variations of the summer 500 hPa GPH and the rainfall anomaly, we applied SVD to the observed fields corresponding to the model hindcast period of 1979–1999. Different

Table 3. The absolute values of correlation coefficients between PCs of three leading observed and model-forecasted EOFs for (a) boreal summer 500 hPa GPH and (b) precipitation anomaly field during 1979–1999. The marked coefficient by one and two asterisks indicates the correlation passed the 0.05 and 0.01 significance testing, respectively.

	Correlation coefficient								
	JMA	GCPS	CWB	MGO	NCEP	IRI	GDAPS	METRI	HMC
(a) 500 hPa GPH anomaly									
PC1	0.79**	0.66**	0.74**	0.71**	0.75**	0.73**	0.67**	0.46*	0.79**
PC2	0.68**	0.13	0.81**	0.50*	0.67**	0.68**	0.66**	0.41	0.18
PC3	0.20	0.23	0.28	0.00	0.01	0.47*	0.07	0.16	0.21
(b) Precipitation anomaly									
PC1	0.65*	0.43*	0.33	0.20	0.29	0.45*	0.04	0.54*	0.44*
PC2	0.01	0.38	0.40	0.04	0.29	0.15	0.06	0.18	0.14
PC3	0.08	0.00	0.07	0.02	0.05	0.05	0.26	0.11	0.36

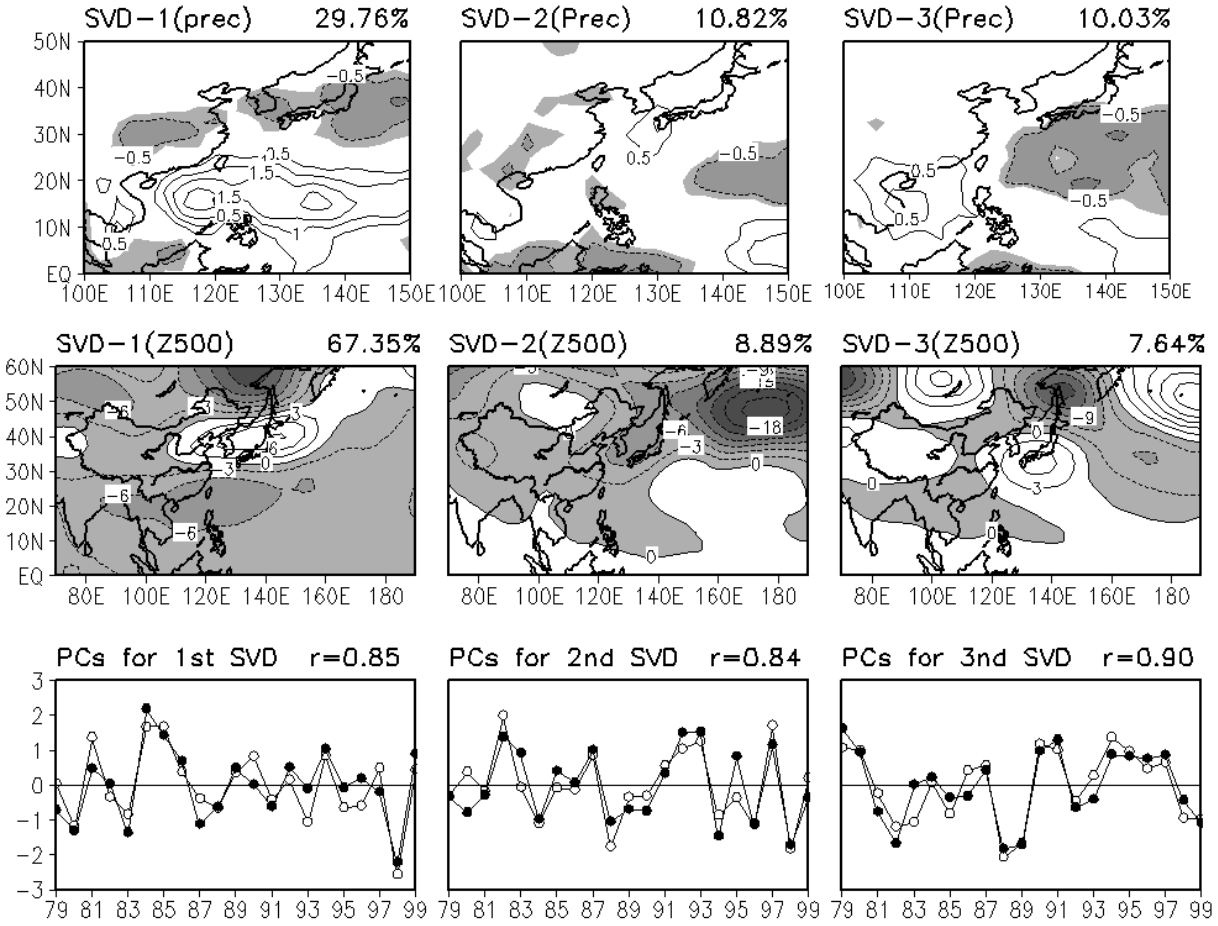

Fig. 8. The three leading SVD modes between the observed summer precipitation anomaly (upper panel; contour interval is 0.5 where the values less than −0.3 are shaded), 500 hPa GPH (middle panel; contour interval is 3 where the negative values are shaded), and their corresponding PCs (bottom panel) during 1979–1999. The solid line with closed and open circle denotes the expansion coefficient for 500 hPa GPH and precipitation anomaly SVD mode, respectively. Squared covariance fraction between two fields is expressed as a percentage and is printed in each title, and the correlation coefficient between the expansion coefficients corresponding to the SVD modes is printed in the bottom title.

from the case of EOF, we choose the domain of precipitation to only be in the study region of 0°–50°N, 100°–150°E. Figure 8 shows the first three SVD modes and expansion coefficients for the observed precipitation and 500 hPa GPH anomaly fields, where we can find that the first pair of SVD modes also show the dominant Pacific-Japan (P–J) patterns similar as the first corresponding EOF counterpart (Fig. 5). The correlation between the expansion coefficients for the first SVD modes reaches 0.85, and it exhibits a close linear relationship between the Asia-Pacific circulation and rainfall anomaly patterns on interannual variability, where the Asia-Pacific summer monsoon precipitation anomaly is dominated by the corresponding circulation anomaly pattern. The enhanced (suppressed) rainfall over the lower middle reaches of the Yangtze River valley to the southern islands of Japan (the SCS to the eastern Philippine Sea) is corresponding to the enhanced (suppressed) 500 hPa GPH anomalies over the corresponding regions, respectively. Meanwhile, the interannual variations of the expansion coefficients show a close relationship with El Niño events. For example, during the summers corresponding to the decaying phase of the El Niño events (Chou et al., 2003), e.g., 1983, 1987, 1991, 1995 and 1998, the rainfall over the low-middle reaches of the Yangtze River valley to the southern Japanese Islands (the SCS to the eastern Philippine Sea) would be greatly enhanced (suppressed).

The coupled relationship is also remarkable in the second and third SVD modes, where the regressed precipitation and 500 hPa GPH anomalies of the SVD modes shows the similar pattern as their corresponding EOF counterparts, and the correlation coefficient

between the expansion coefficients for the second and third SVD modes is 0.84 and 0.90, respectively. In addition, we found that the correlations between the three expansion coefficients corresponding to the EOF and SVD modes with respect to the precipitation and 500 hPa GPH anomalies range from 0.82 to 0.99, which passed the 0.01 significance test.

5. A statistical downscaling scheme and its forecasting skill

5.1 *Statistical downscaling scheme*

The models show better performance in predicting the 500 hPa GPH anomaly field. However, the models are either producing centers of variability in geographical positions away from the corresponding observed positions or the models are missing some centers of variability. Such errors may degrade the skill of the model if the skill score is based on grid point comparisons between predictions and observations, which is very common (Feddersen et al., 1999; Kang et al., 2004). These model systematic errors are mainly related to the spatial pattern shift, whereas, such errors can be corrected on the basis of the linear regression between the expansion coefficients corresponding to the eigenmodes of observation and model prediction during a training period based on either EOF or SVD (e.g., Feddersen et al., 1999; Kang et al., 2004; Yun et al., 2005).

In the present study, we use the EOF scheme to correct model systematic error in predicting the spatial pattern of the 500 hPa GPH anomaly field following the same procedure as described by Yun et al. (2005), where each model forecast is corrected by using a combination of the past observations and the model forecasts, and a consistent spatial pattern is determined among the observations and forecasts using a linear regression relationship in the EOF space.

In this study, the training period is 19 yr, and the remaining 2 yr are used for target forecast and verification. The time series of observation of $X(x,t)$ during a training period of t and model forecasts of $F(x,t+\Delta t)$ during the whole period of $t+\Delta t$ can be written as a linear combination of EOFs such as,

$$X(x,t) = \sum_{i=1}^{n} P_i(t) \cdot \phi_i(x) \,, \tag{1}$$

$$F(x,t+\Delta t) = \sum_{i=1}^{n} Q_i(t+\Delta t) \cdot \varphi_i(x) \,. \tag{2}$$

Here, index i and n in Eqs. (1) and (2) represent the particular EOF and the retained number of EOF modes, respectively. $P_i(t)$ and $\phi_i(x)$ are the i-th principal component (PC) and the corresponding EOF mode for the observed field during a training period, $Q_i(t+\Delta t)$ and $\varphi_i(x)$ have the same meanings but for the model forecast of $F(x,t+\Delta t)$, which covers the training and model forecast time period. Using a regression relationship between the PC time series between observation and model forecast data, it is possible to reduce the spatial pattern shift of model forecast errors, which evolves in a consistent way with the EOFs of the observation for the time series considered. A number of linear regression relationships between $P_i(t)$ and $Q_i(t+\Delta t)$ during a training period are given by

$$\tilde{P}_i(t) = a_i Q_i(t) + \varepsilon_i \,, \quad i = 1, \ldots, n \,, \tag{3}$$

where, $\tilde{P}_i(t)$ is the regressed PC of $P_i(t)$ and ε_i is the residual. The regression coefficients of a_i are calculated when the residual error variance of $E(\varepsilon_i^2)$ is minimized. According to these linear regression relationships, the corrected model forecast PC of the i-th EOF mode at the target year can be expressed by

$$\tilde{P}_{i,\mathrm{reg}}(t+\Delta t) = a_i Q_i(t+\Delta t) \,, \quad i = 1, \ldots, n \,. \tag{4}$$

Therefore, the corrected model forecast of $\tilde{F}(x,t+\Delta t)$ at the target year can be constructed by the combination of observed EOF modes and corrected model forecasted PC, which is given by

$$\tilde{F}(x,t+\Delta t) = \sum_{i=1}^{n} \tilde{P}_{i,\mathrm{reg}}(t+\Delta t) \cdot \phi_i(x) \,. \tag{5}$$

The model-forecasted precipitation anomalies could be downscaled by the transfer function explored by SVD, which is constructed on the basis of model-forecasted 500 hPa GPH after correction and the observed precipitation anomaly fields during a training time period. Suppose during a training period, the model-forecasted 500 hPa GPH and the observed precipitation anomaly fields are represented by $Z(x,t)$ and $Y(x,t)$, then they can be decomposed by the expansion coefficients and the corresponding SVD modes as:

$$Z(x,t) = \sum_{\mathrm{j}=1}^{m} u_j(t) \cdot g_j(x) \,, \tag{6}$$

$$Y(x,t) = \sum_{\mathrm{j}=1}^{m} v_j(t) \cdot h_j(x) \,. \tag{7}$$

Here, the two fields are normalized to have mean zero and standard deviation at each grid point, the index j is the particular SVD mode and m is the total number of retained SVD modes ($m \leqslant n$). The patterns of $g_i(x)$ and $h_i(x)$ are corresponding to the j-th pair of SVD modes between the two anomaly fields, $u_j(t)$ and

$v_j(t)$ are time series of expansion coefficients, which are calculated by the projections of $Z(x,t)$ and $Y(x,t)$ onto the singular vectors explored by SVD (Feddersen et al., 1999; Feddersen, 2003). Similar to Eq. (3), the linear regression relationship between $u_j(t)$ and $v_j(t)$ can be constructed as follows:

$$\tilde{v}_j(t) = \beta_j u_j(t) + \varepsilon_j \ , \quad j = 1, \ldots, m \ , \tag{8}$$

where, ε_j is the residual, β_j are the linear regression coefficients between $u_j(t)$ and $v_j(t)$ corresponding to the j-th pair of SVD modes, which are calculated when the residual error variance of $E(\varepsilon_j^2)$ is minimized. Then, the forecasted time series of $u_j(t+\Delta t)$ corresponding to the model j-th SVD mode at the target forecast year can be defined as:

$$\tilde{u}_j(t+\Delta t) = \tilde{F}(x, t+\Delta t) \cdot g_j(x) \ , \ \ j = 1, \ldots, m \ , \tag{9}$$

where, $\tilde{F}(x, t+\Delta t)$ is given by Eq. (5). According to Eq. (7), the forecasted $\tilde{Y}(x, t+\Delta t)$ of the model precipitation at the target year can be written as:

$$\tilde{Y}(x, t+\Delta t) = \sum_{j=1}^{m} \beta_j \tilde{F}(x, t+\Delta t) \cdot g_j(x) \cdot h_j(x) \ . \tag{10}$$

Therefore, the downscaled precipitation anomaly forecast of $\tilde{Y}(x, t+\Delta t)$ is jointly decided by the linear regression coefficient β_j and the corrected model forecast of $\tilde{F}(x, t+\Delta t)$.

It is noted that the transfer function linking the 500 hPa GPH of the models and the observed precipitation anomaly fields is constructed by the linear regression between the leading expansion coefficients corresponding to the SVD modes during a training time period where the dominant SVD modes between two anomaly fields can be explained as the dominant circulation and precipitation anomaly patterns, which control the summer climate anomaly over the Asia-Pacific region.

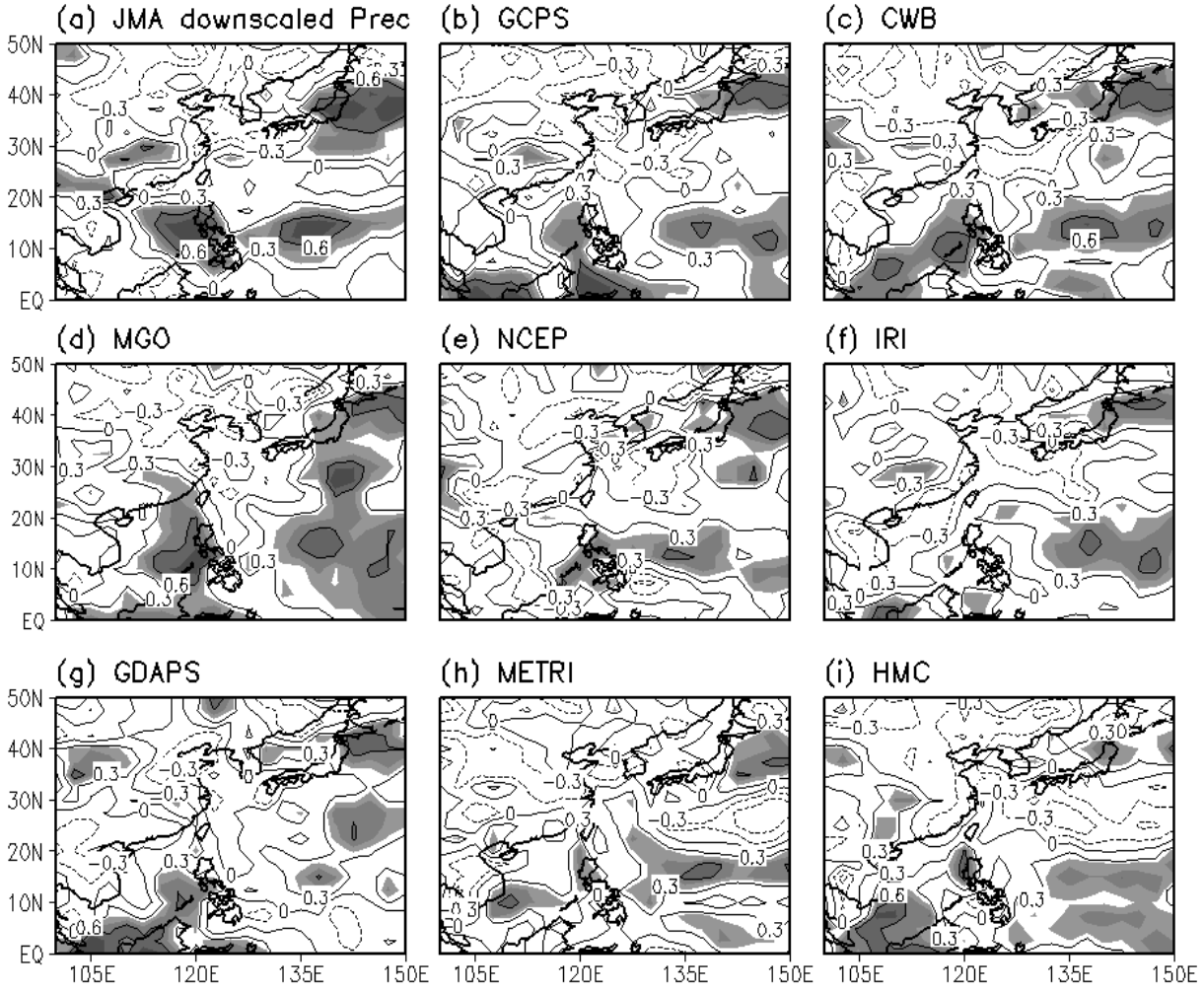

Fig. 9. Same as Fig. 1, except for the downscaled precipitation anomaly forecasts.

5.2 *Forecasting skill scores*

According to this statistical downscaling scheme, the success of the Asia-Pacific summer monsoon rainfall anomaly forecast is dependent on the model forecast of 500 hPa GPH anomaly and the transfer function. To examine the skill of this statistical downscaling rainfall anomaly forecast, we retain the first three leading EOF and SVD corresponding modes based on the evaluation of the models' predictions and apply this scheme to all models. We consider the first 19-yr as the training period and the last two year as the target years for the Asia-Pacific summer rainfall downscaling forecast. In order to avoid the over-fitting in this downscaling scheme, we used the cross validation to examine this downscaling forecasting skill following the previous studies (e.g., Feddersen et al., 1999; Kang et al., 2004; Yun et al., 2005), where the EOF and SVD are repeatedly applied to the data sets from which the observations at the target year are excluded. This is similar to the previous definition, but the MME is defined, by this downscaling scheme, as the simple composite of downscaled precipitation anomaly fields in the nine different models.

This downscaling scheme shows better performance in improving the model forecast skill of the summer monsoon rainfall anomaly in the Asia-Pacific region (Fig. 9). It is found that the correlations between the downscaled rainfall anomalies in the models and the observation have been significantly improved in the lower-middle reaches of the Yangtze River, the southern islands of Japan, the SCS to the eastern Philippine Sea, and the western North Pacific region, where the Asia-Pacific summer monsoon prevails associated with the rain bands of mei-yu-Changma-Baiu. In these areas, the correlation coefficients range from 0.2 to 0.8

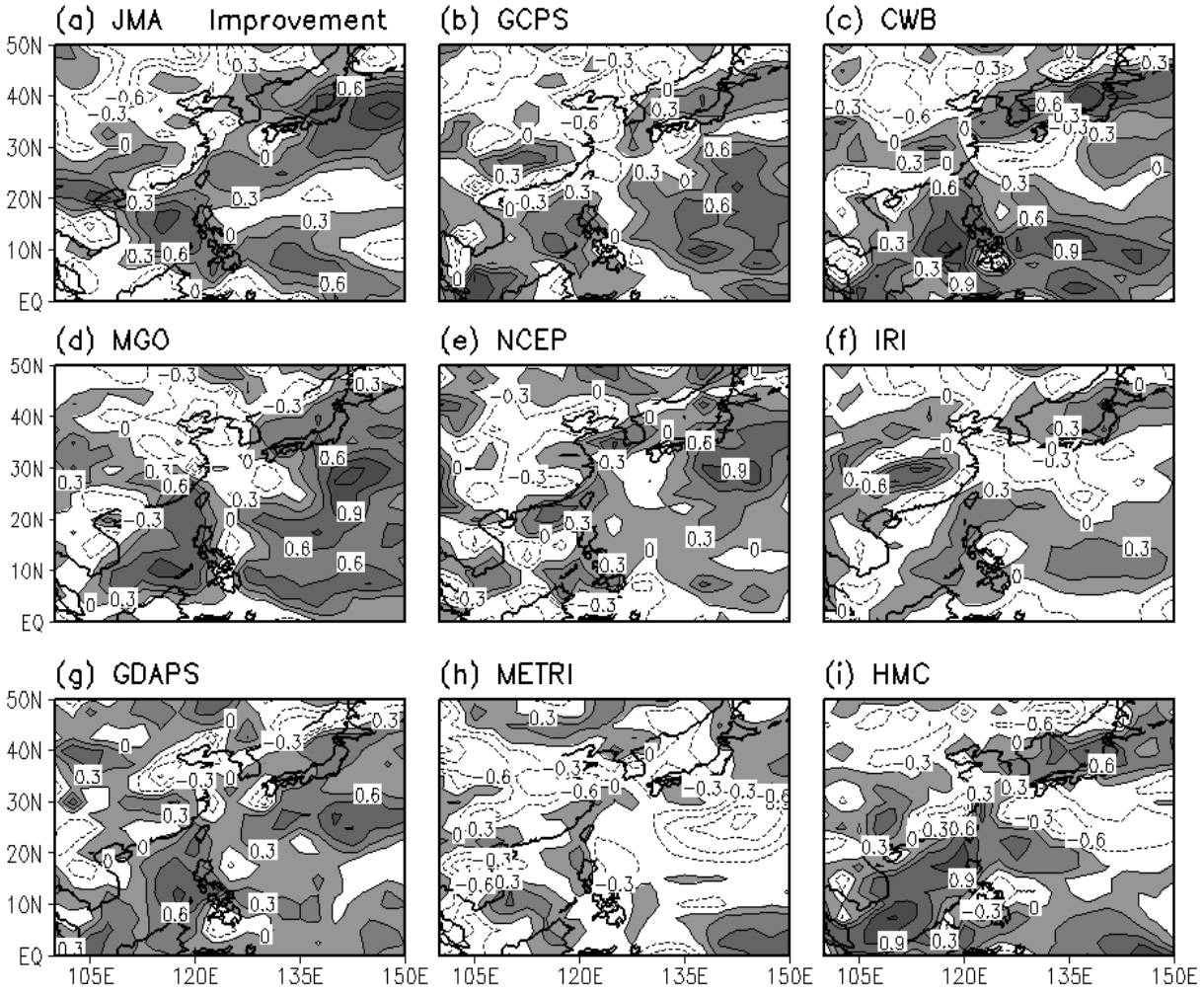

Fig. 10. The differences of correlation coefficients between the model-predicted and downscaled precipitation anomaly against the observation during 1979–1999 for (a) JMA, (b) GCPS, (c) CWB, (d) MGO, (e) NCEP, (f) IRI, (g) GDAPS, (h) METRI, and (i) HMC models. Contour interval is 0.3 and the positive values are shaded.

in most models comparing to the weak and even the negative correlations in the original model predictions (see Fig. 1). Figure 10 shows the differences of correlation coefficients between the model-predicted and the downscaled rainfall anomaly forecasts based on 21-yr cross-validations, where the positive and negative values show the improved and degraded forecasting skill scores. In association with the positive correlations, the improved forecasting skills by this downscaling scheme also can be observed in the models, where the positive values dominate the Asia-Pacific summer monsoon prevailing areas and the maximum exceeds 0.9.

To examine the year-to-year forecasting skill of summer monsoon rainfall anomaly by this downscaling scheme, we calculated the ACC and the RMSE of downscaled rainfall anomaly in each model and MME prediction over the same region of (0°–50°N, 100°–150°E) as defined in section 2 (see Fig. 11). The 21-yr forecasts show that this downscaling scheme has a better forecasting capability for each model and MME scheme, and its good performance is substantially shown during 1979–1999 except in 1980. It exhibits a weaker performance in 1980 when the ACC in 6 of the 9 models were severely degraded during this summer. A similar situation can also be found in 1989 and 1995, but in fewer models, which suggests that the rainfall pattern anomaly is less predictable for the summer corresponding to non-ENSO years when the Asia-Pacific summer monsoon anomaly is dominated by the meridional temperature gradient in the upper troposphere (Chou et al., 2003). It was observed that the summer rainfall anomaly forecast skill in the Asia-Pacific monsoon region is generally improved by this downscaling scheme in the models, where the averaged ACC of downscaled rainfall anomaly fields during 1979–1999 ranges from 0.13 to 0.27 in contrast to the original range of −0.05 to 0.18 of the model-predicted rainfall anomaly fields after downscaling.

Figure 11 shows that the averaged ACC and RMSE in the MME prediction by this downscaling scheme during 1979–1999 is 0.24 and 1.55 mm d^{-1} in contrast to 0.07 and 1.73 mm d^{-1} in the old MME forecast based on the model-predicted precipitation anomaly fields. To examine how well this downscaling scheme works, we calculated the 21-yr correlation coefficients of the MME predictions, respectively based on the model-predicted and downscaled rainfall anomaly fields against the observed counterpart, and presented the results in Fig. 12. Here, we can clearly see that this downscaling scheme does improve the summer rainfall anomaly forecast skill in the MME prediction, particularly over the SCS to the eastern Philippine Sea, the lower-middle reaches of the Yangtze River valley to central Japan, and the major parts of the northwestern Pacific region, where the correlation coefficients of

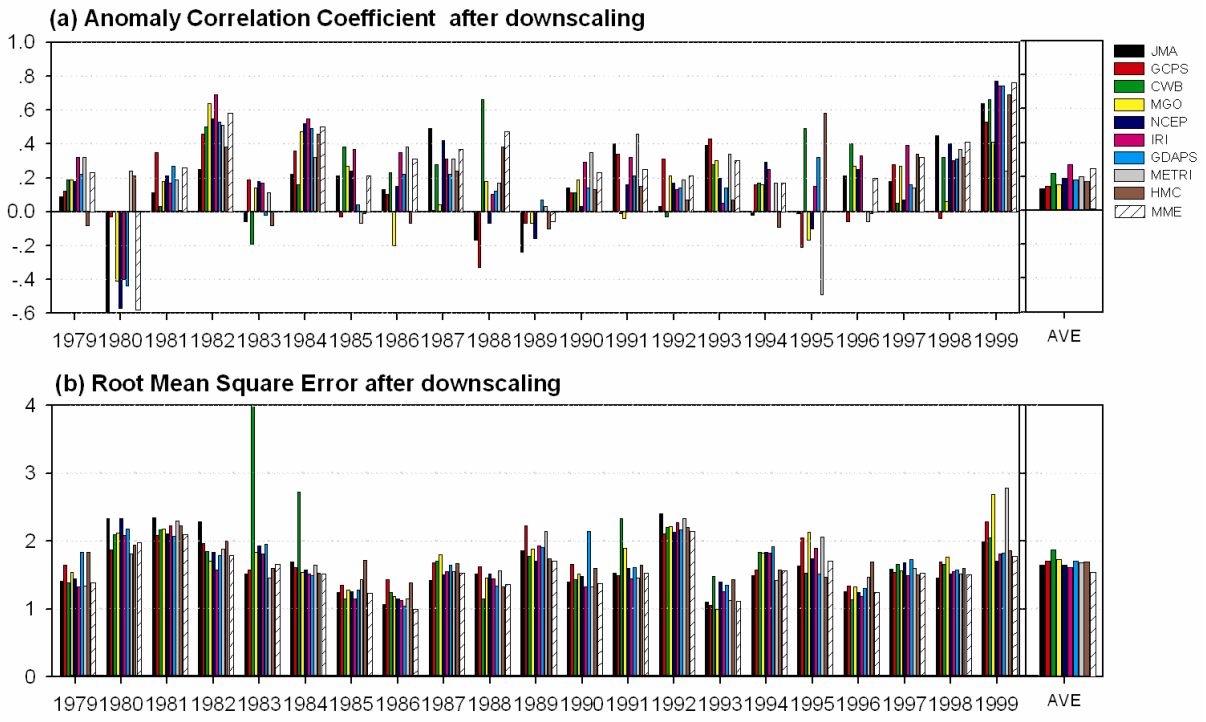

Fig. 11. Same as Fig. 2, except for the downscaled precipitation anomaly fields.

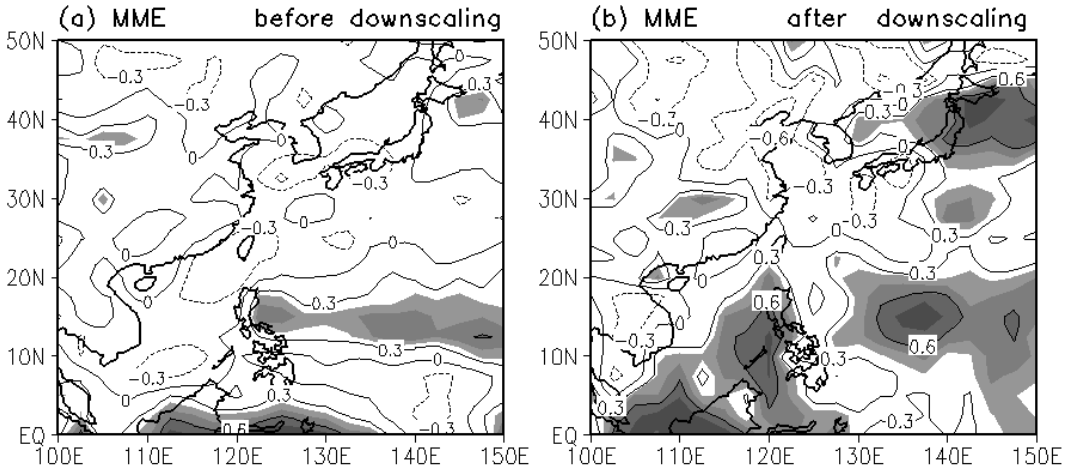

Fig. 12. Correlation coefficients between observed and MME-predicted precipitation anomaly for 21-yr (a) before and (b) after downscaling. Contour interval is 0.3, the regions where the values greater than 0.1 are shaded. The enclosed region by the thick line indicates where the correlations passed the 0.05 significance test level.

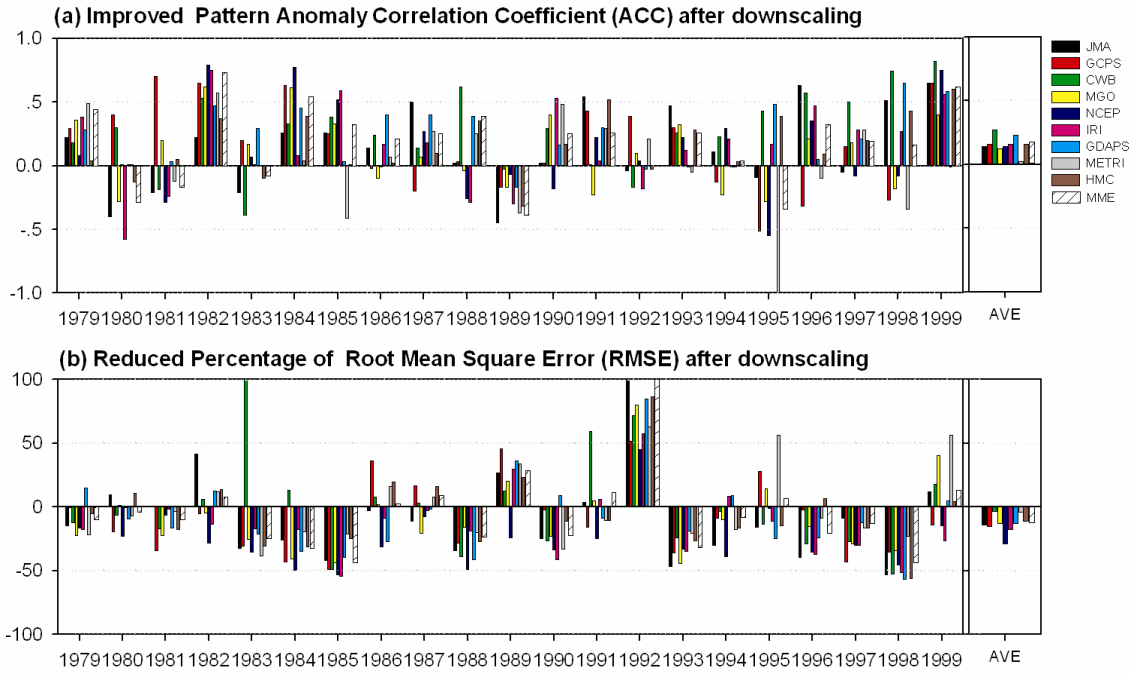

Fig. 13. The improved forecasting skill scores of ACC and RMSE by the downscaling scheme in the models and the MME predictions during 1979–1999.

the summer rainfall anomalies range from 0.2 to 0.8 in contrast to the negative correlation coefficients in the old MME prediction. The MME forecast, even based on a simple composite of the multi-model ensemble predictions, may improve the rainfall anomaly forecast skill scores exhibited in the ACC and the RMSE compared to the individual model forecast. However, it should be noted that it has limited capability to correct the model forecast errors and improve the forecast skill in some common regions, where the models show weaker forecasting performance.

The improvement of Asia-Pacific summer rainfall anomaly forecasts in the models and MME prediction by this downscaling scheme can be evaluated by the differences between the ACCs and RMSEs of rainfall anomaly fields before and after downscaling in Fig. 13,

where the positive values of ACC differences are found in many cases of year-to-year predictions corresponding to the negative values of RMSE differences in the models. In contrast to the cases of model predictions, the improved ACC ranges from 0.02 to 0.27 in the models, corresponding to the improved RMSE varying from 4% to 29%. The summer rainfall anomaly bands in the Asia-Pacific region have been well predicted in the MME forecast although less improvement of ACC and RMSE is found in MME prediction as we have discussed. Therefore, this downscaling scheme generally exhibits a good performance in improving the summer rainfall anomaly forecast, particularly for those models where the monsoon circulation was well predicted and the MME prediction was as well.

6. Summary and concluding remarks

The dynamic seasonal prediction is mainly based on the assumption that the climate variation is dominated by the slowly varying boundary conditions, particularly the interannual variability of large-scale SST anomalies. Therefore, the accurate seasonal predictions depend upon the correct response of the model atmosphere to the external SST anomaly forcing. In this study, we evaluated the 9 model performances in the seasonal prediction of Asia-Pacific summer monsoon rainfall and circulation anomalies, and proposed a statistical downscaling scheme to improve the prediction skill of the summer monsoon rainfall anomalies in the Asia-Pacific region.

On the basis of 21-yr ensemble predictions in 9 different GCMs, we found that the models have shown different skill scores in the seasonal prediction of atmospheric variables in the Asia-Pacific summer monsoon region. For example, the models can capture the 500 hPa GPH better than the precipitation anomaly. However, the summer monsoon circulation and precipitation anomalies in the models' predictions are not matching well. The models show the capability in predicting the interannual variability of the Asia-Pacific summer monsoon circulation anomaly represented by the WNPMI, but they failed to forecast the relationship between WNPMI and precipitation anomaly in the middle-higher latitudes of East Asia and the western North Pacific region, due to the spatial pattern shift in the model predictions.

In contrast to the rainfall anomaly field forecasts, models can well predict the interannual variability of PCs of the 500 hPa GPH anomaly fields but show unrealistic EOF patterns. According to this model forecasting performance and the coupled relationship between the 500 hPa GPH and precipitation anomaly fields in the Asia-Pacific region, we proposed a statistical downscaling scheme for the summer rainfall anomaly forecast. In this scheme, the three leading EOF modes of 500 hPa GPH anomaly fields predicted by the models are first corrected by the linear regression between the principal components in each model and observation, respectively. Then, the corrected GPH anomaly in the models is chosen as the predictor to downscale the precipitation anomaly field, which is assembled by the forecasted expansion coefficients of model 500 hPa GPH and the three leading SVD modes of observed precipitation anomaly corresponding to the prediction of model 500 hPa GPH during a 19-yr training time period. The cross-validated forecasts suggest that this downscaling scheme may have the potential to improve the forecast skill of the precipitation anomaly in the Asia-Pacific region for the models and the conventional multi-model ensemble prediction, where the summer monsoon rain bands anomalies can be well predicted, and the root mean square errors have been substantially reduced by this downscaling scheme. However, we found that the statistical downscaling scheme did not show a good performance in any area. For instance, over the triangle ocean areas among China, Korea, and Japan, the downscaled precipitation anomaly forecast skill scores are still lower; this might be related to the monsoon synoptic and typhoon influences. These rainfall anomalies could not be produced in either an AGCM or in this downscaling scheme.

The success of downscaling forecast depends not only on the skill of the downscaling method, but also on the quality of the predictions provided by the models. The current widely applied statistical downscaling schemes are mainly constructed on the relationship between the variations of observation and model forecast explored by CCA, EOF, and SVD. These methods only document the variability of model forecast rather than the model dynamics (Zwiers and von Storch, 2004), therefore, the real dynamic performance of the models may not be evaluated by these statistical analyses.

Acknowledgements. The authors would like to thank the Asia-Pacific Economic Cooperation (APEC) members for providing the data of the model predictions used in this present study. The National Natural Science Foundation of China (NSFC), Grant Nos. 90711003, 40375014, the program of GYHY200706005, and the APCC Visiting Scientist Program jointly supported this work.

REFERENCES

Brankovic, C., T. N. Palmer, and L. Ferranti, 1994: Predictability of Seasonal Atmospheric Variations. *J. Climate*, **7**, 217–237.

Charles, S. P., B. C. Bates, P. H. Whetton, and J. P. Hughes, 1999: Validation of downscaling models for changed climate conditions: Case study of southwestern Australia. *Climate Research*, **12**, 1–14.

Chou, C., J. Tu, and J. Yu, 2003: Interannual Variability of the Western North Pacific Summer Monsoon: Differences between ENSO and Non-ENSO Years. *J. Climate*, **16**, 2275–2287.

Feddersen, H., 2003: Predictability of seasonal precipitation in the Nordic region. *Tellus*, **55A**, 385–400.

Feddersen, H., A. Navarra, and M. N. Ward, 1999: Reduction of model systematic error by statistical correction for dynamical seasonal prediction. *J. Climate*, **12**, 1974–1989.

Goswami, B. N., 1998: Interannual variations of Indian summer monsoon in a GCM: External conditions versus internal feedbacks. *J. Climate*, **11**, 501–522.

Hagedorn, R., R. F. J. Doblas-Reyes, and T. N. Palmer, 2005: The rationale behind the success of multimodel ensembles in seasonal forecasting—I. Basic concept. *Tellus*, **57A**, 219–233.

Kang, I.-S., and Coauthors, 2002: Intercomparison of the climatological variations of Asian summer monsoon precipitation simulated by 10 GCMs. *Climate Dyn.*, **19**, 383–395.

Kang, I.-S., J.-Y. Lee, and C.-K. Park, 2004: Potential predictability of a dynamical seasonal prediction system with systematic error correction. *J. Climate*, **15**, 834–844.

Kanamitsu, M., W. Ebisuzaki, J. Woollen, S.-K. Yang, J. J. Hnilo, M. Fiorion, and G. L. Potter, 2002: NCEP-DOE AMIP-II Reanalysis (R-2). *Bull. Amer. Meteor. Soc.*, **83**, 1631–1643.

Kusunoki, S., M. Sugi, A. Kitoh, C. Kobayashi, and K. Takano, 2001: Atmospheric seasonal predictability experiments by the JMA AGCM. *J. Meteor. Soc. Japan*, **79**, 1183–1206.

Lee, E.-J., J.-G. Jhun, and C.-K. Park, 2005: Remote connection of the East-Asian summer rainfall variation revealed by a newly defined monsoon index. *J. Climate*, **18**, 4381–4393.

Li, J., and Q. Zeng, 2002: A unified monsoon index. *Geophys. Res. Lett.*, **28**(8), 10.1029/2001GL013874.

Nitta, T., 1987: Convective activities in the tropical western Pacific and their impact on the Northern hemisphere summer circulation. *J. Meteor. Soc. Japan*, **65**, 373–390.

Nitta, T., and Z.-Z. Hu, 1996: Summer climate variability in China and its association with 500 hPa height and tropical convection. *J. Meteor. Soc. Japan*, **74**, 425–445.

Palmer, T. N., C. Brankovic, and D. S. Richardson, 2000: A probability and decision-model analysis of PROVOST seasonal multi-model ensemble integrations. *Quart. J. Roy. Meteor. Soc.*, **126**, 2035–2067.

Slingo, J. M., and Coauthors, 1996: Intraseasonal oscillations in 15 atmospheric general circulation models: results from an AMIP diagnostic subproject. *Climate Dyn.*, **12**, 325–357.

Sperber, K. R., and T. N. Palmer, 1996: Interannual tropical rainfall variability in general circulation model predictions associated with the Atmosphere Model Intercomparison Project. *J. Climate*, **9**, 2727–2750.

Sperber, K. R., and Coauthors, 2001: Dynamical Seasonal Predictability of the Asian Summer Monsoon. *Mon. Wea. Rev.*, **129**, 2226–2248.

Tao, S. Y., and L.-X. Chen, 1987: A review of recent research on the East Asian summer monsoon in China. *Monsoon Meteorology*, C. P. Chang and T. N. Krishnamurti, Eds., Oxford University Press, 60–92.

Wang, B., and Z. Fan, 1999: Choice of South Asian summer monsoon indices. *Bull. Amer. Meteor. Soc.*, **80**, 629–638.

Wang, B., R. Wu, and K. M. Lau, 2001a: Interannual variability of the Asian summer monsoon: Contrasts between the Indian and the western North Pacific-East Asian monsoons. *J. Climate*, **14**, 4073–4090.

Wang, B., I.-S. Kang, and J.-Y Lee, 2004: Ensemble predictions of Asian-Australian monsoon variability by 11 AGCMs. *J. Climate*, **17**, 803–818.

Wang, G., R. Kleeman, N. Smith, and F. Tseitkin, 2001b: The BMRC coupled general circulation model ENSO forecast system. *Mon. Wea. Rev.*, **130**, 975–991.

Wilby, R. L., and T. M. L. Wigley, 2000: Precipitation predictors for downscaling: Observed and General Circulation Model relationships. *International Journal of Climatology*, **20**, 641–661.

Yun, W. T., L., Stefanova, A. K., Mitra, T. S., vijaya Kumar, W. Dewar, and T. N. Krishnamurti, 2005: A multimodel superensemble algorithm for seasonal climate prediction using DEMETER forecast. *Tellus*, **57A**, 1–10.

Xie, P., and P. A. Arkin, 1997: Global precipitation: A 17-year monthly analysis based on gauge observations, satellite estimates, and numerical model outputs. *Bull. Amer. Meteor. Soc.*, **78**, 2539–2558.

Zhu, C., W. Lee, H. Kang, and C. Park, 2005: A proper monsoon index for seasonal and interannual variations of the East Asian monsoon. *Geophys. Res. Lett.*, **32**, L02811, doi:10.1029/2004GL021295.

Zwiers, F., and H. von Storch, 2004: On the role of statistics in climate research. *International Journal of Climatology*, **24**, 665–680.